SUPPLEMENT

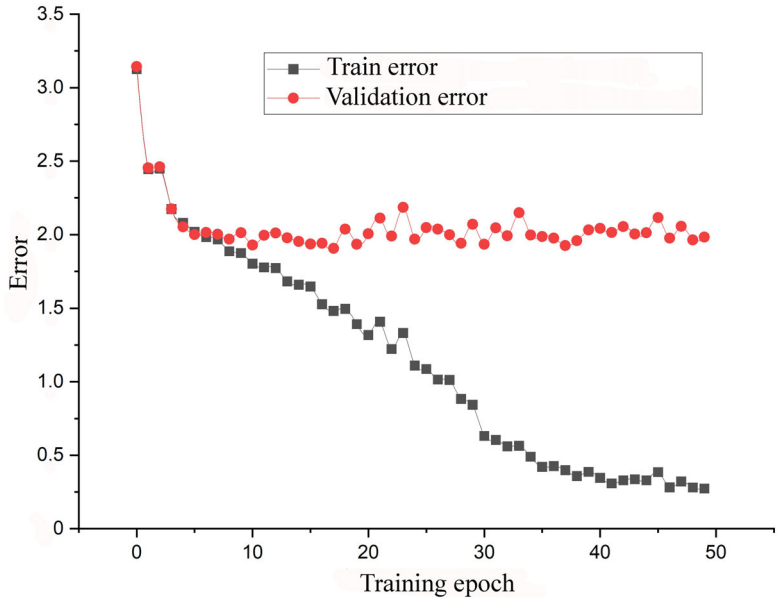

Fig. S1. Training curves of the Pafnucy neural network on the PDBbind2020 set. For modeling, the coefficients of the 25th epoch were selected.

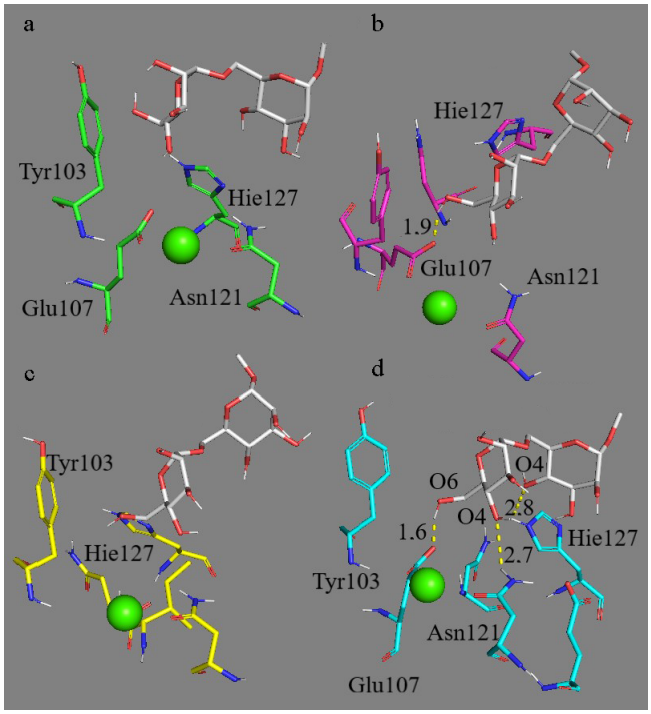

Fig. S2. Modeling of dimannose **8** binding by the domain of the mannose receptor CD206. The following complexes are shown: the initial arrangement (a) and the arrangement after 10-ns (b), 30-ns (c), and 250-ns (d) molecular dynamics simulation. The green sphere is Ca^{2+}.

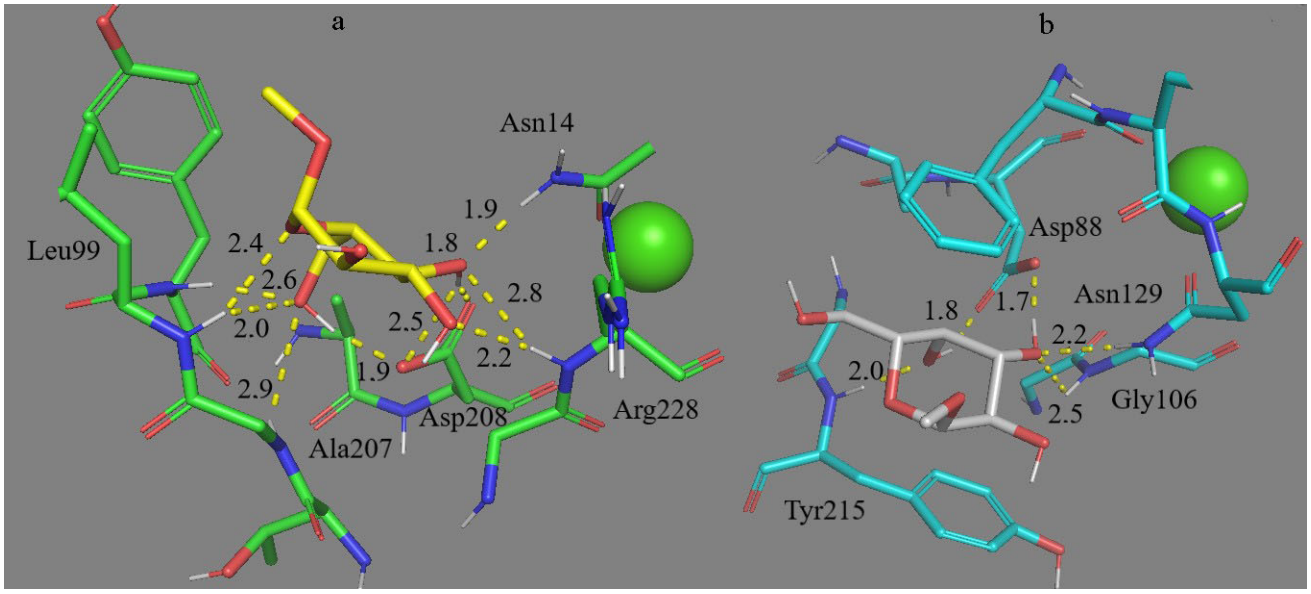

Fig. S3. Spatial structures of ConA complexes with monosaccharides: a) methyl-α-D-glucopyranoside **12** (yellow); b) methyl-α-D-galactopyranoside **13** (white). The green sphere is Ca^{2+}. Molecular dynamics within 10 ns.

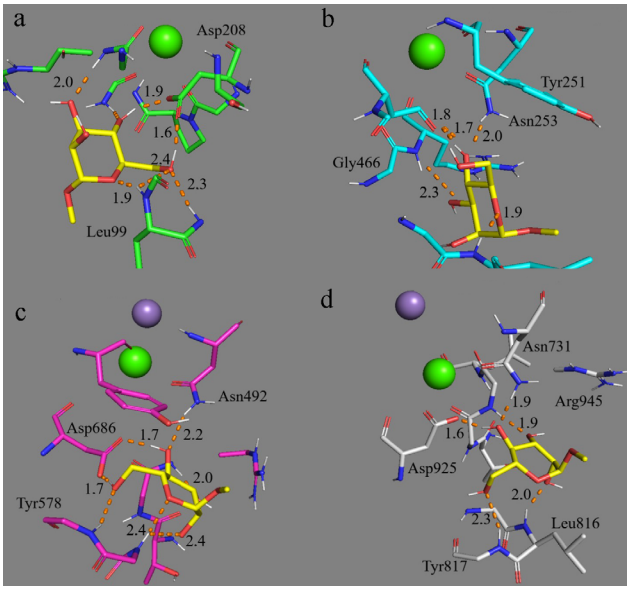

Fig. S4. Spatial structures of the ConA subunit complexes with methyl-α-D-mannoside **2** (shown in yellow): a) Subunit A; b) subunit B; c) subunit C; d) subunit D. The green sphere is Ca^{2+}. Molecular dynamics within 10 ns.

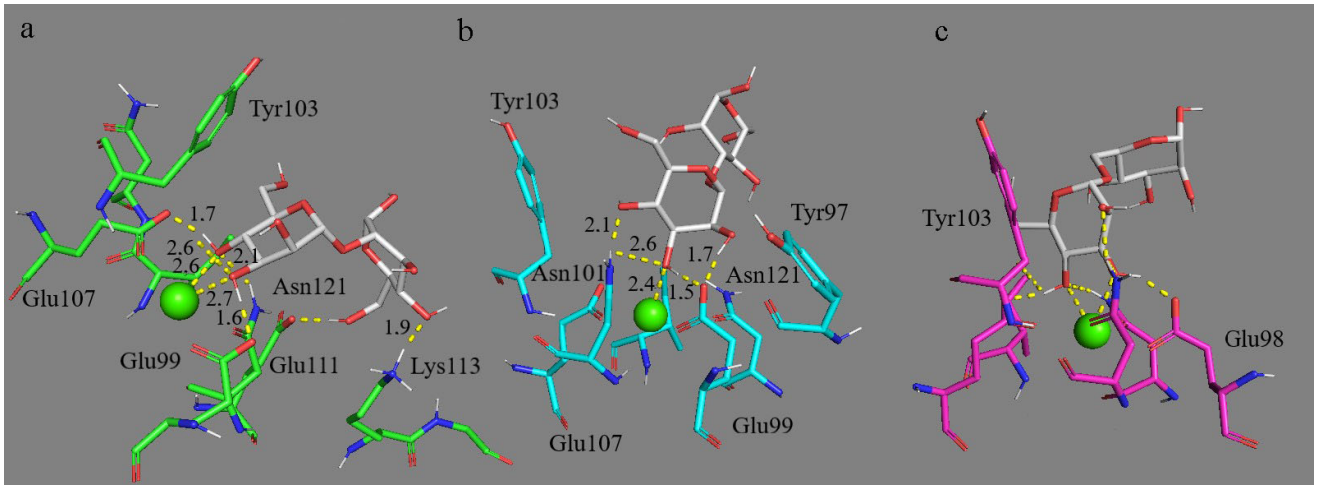

Fig. S5. Effect of the glycoside type on dimannose binding by the fourth domain of the mannose receptor CD206. a) α(1,2)-dimannopyranoside **4**; b) α(1,3)-dimannopyranoside **6**; c) α(1,6)-dimannopyranoside **7**. 100-ns molecular dynamics simulation.

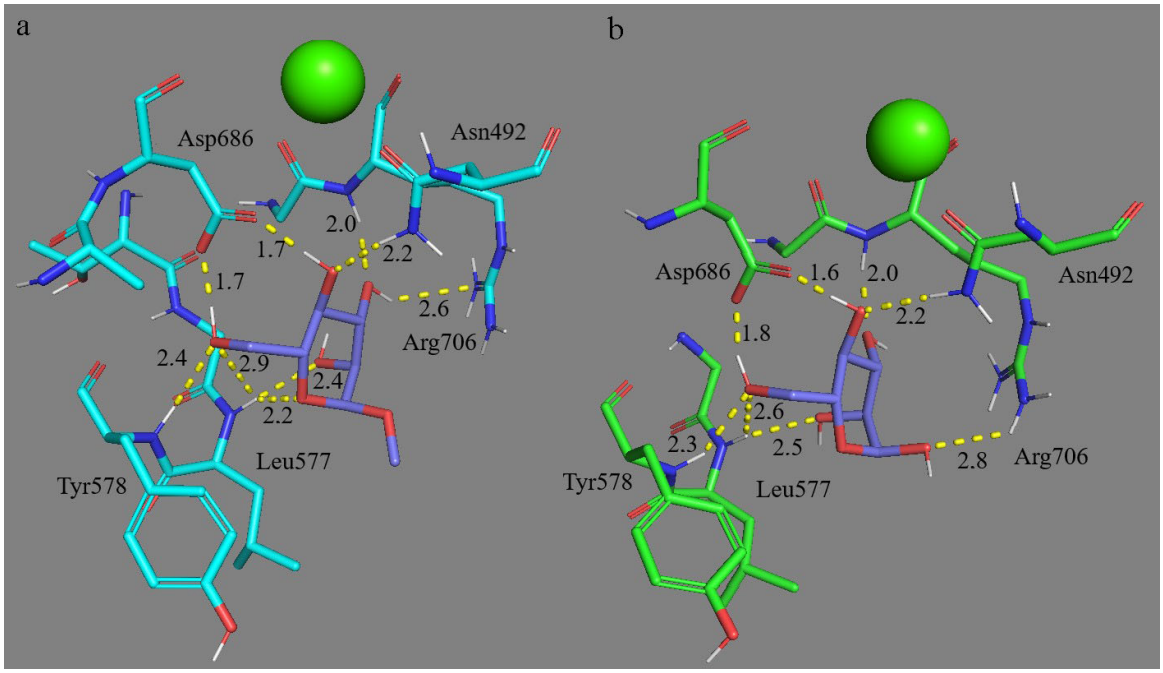

Fig. S6. Effect of the O1 atom methylation on binding mannose by concanavalin A. a) α-Mannose **1** [PDB – 5CNA]; b) Me-α-mannopyranoside **2** [PDB – 5CNA]. 10-ns molecular dynamics simulation.

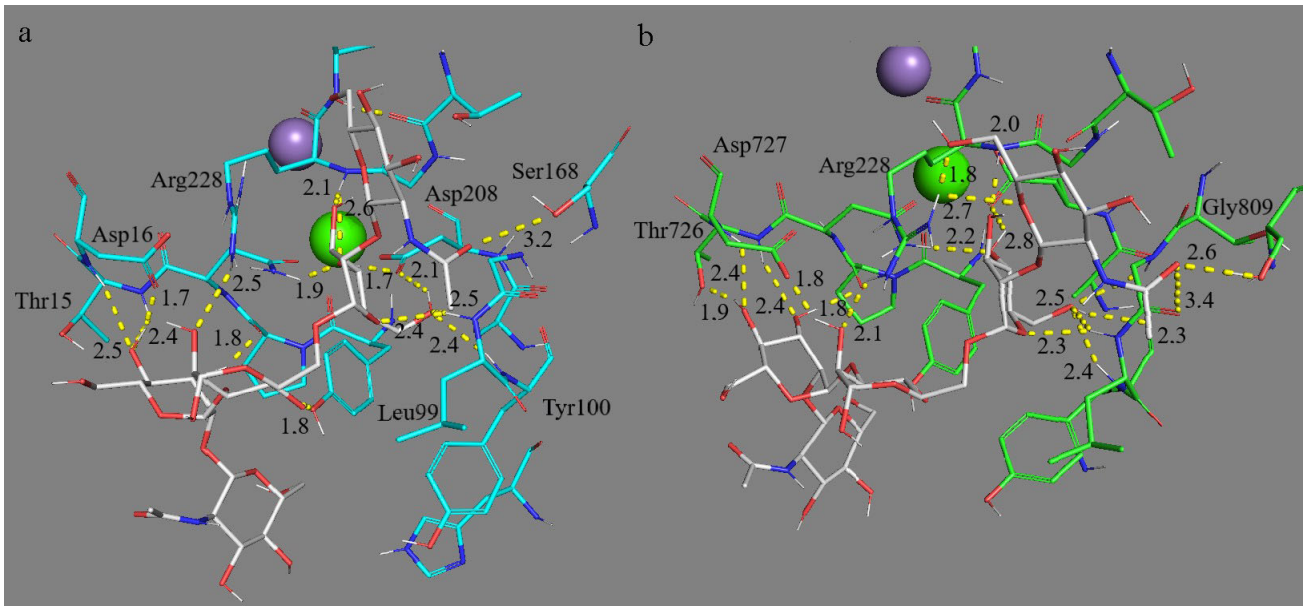

Fig. S7. Spatial structures of ConA subunit complexes with 3,6-di-O-(β(1,2)-N-acetylglucosamino-mannopyranosyl)-α-mannopyranose **11** [PDB – 1TEI] (shown in white): Subunit A (a); subunit D (b). The green sphere is Ca^{2+}, the purple sphere is Mn^{2+}. 10-ns molecular dynamics simulation.

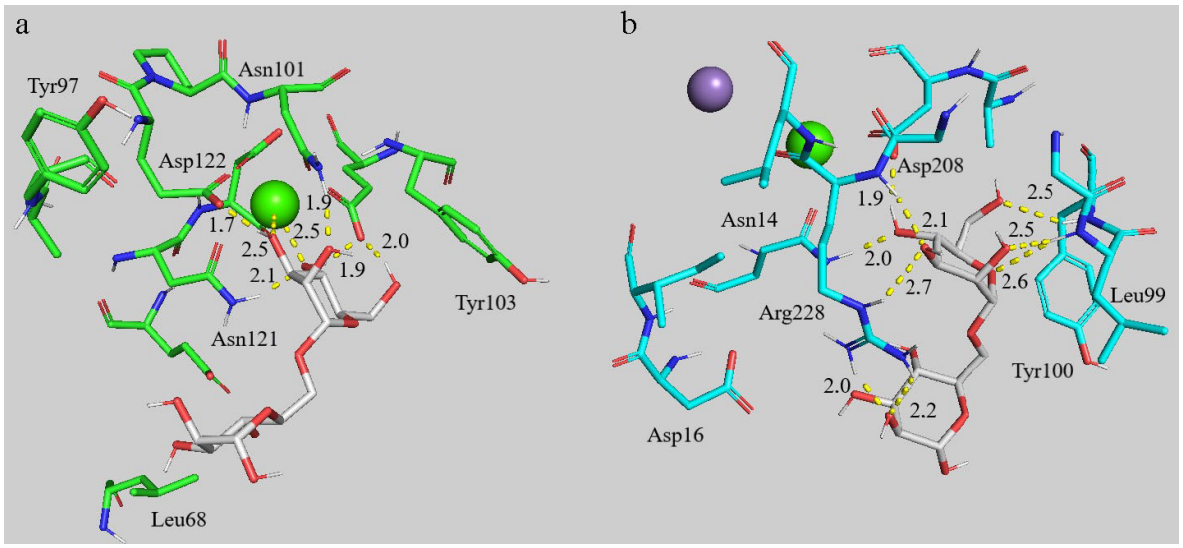

Fig. S8. Spatial structures of complexes of α(1,6)-dimannopyranoside **7** with the fourth domain of the mannose receptor CD206 (a) and with ConA (b). 10/100-ns molecular dynamics simulation.